

## RESEARCH PAPER

## Synthesis of 2,3-dihydroperimidines in the Presence of Nano- $\gamma$ - $\text{Al}_2\text{O}_3/\text{BF}_n$ and Nano- $\gamma$ - $\text{Al}_2\text{O}_3/\text{BF}_n/\text{Fe}_3\text{O}_4$ as Catalysts under Different Conditions

Asma Mazoochi<sup>1</sup>, Abdolhamid Bamoniri<sup>2\*</sup>, Seied Ali Pourmousavi<sup>1</sup>

<sup>1</sup> School of Chemistry, Damghan University, Damghan, I.R. Iran

<sup>2</sup> Department of Organic Chemistry, Faculty of Chemistry, University of Kashan, Kashan, I.R. Iran

## ARTICLE INFO

**Article History:**

Received 02 March 2021

Accepted 05 June 2021

Published 01 July 2021

**Keywords:**

2,3-Dihydroperimidines

Aromatic aldehydes

Heterogeneous catalyst

Nano- $\gamma$ - $\text{Al}_2\text{O}_3/\text{BF}_n$

Nano- $\gamma$ - $\text{Al}_2\text{O}_3/\text{BF}_n/\text{Fe}_3\text{O}_4$

Naphthalene-1,8-diamine

## ABSTRACT

Lewis acid heterogeneous nano catalysts entitled nano- $\gamma$ - $\text{Al}_2\text{O}_3/\text{BF}_n$  and nano- $\gamma$ - $\text{Al}_2\text{O}_3/\text{BF}_n/\text{Fe}_3\text{O}_4$  were prepared and characterized using Fourier transform infrared (FT-IR), Vibrating-sample magnetometer (VSM), X ray diffraction (XRD), Transmission electron microscope (TEM), Thermal gravimetric analysis (TGA), Field emission-scanning electron microscopy (FE-SEM), Energy-dispersive x-ray spectroscopy (EDS) and Brunauer–Emmett–Teller (BET) techniques. These highly effective heterogeneous catalysts have been used for the synthesis of substituted perimidines *via* reaction of naphthalene-1,8-diamine with various aromatic aldehydes under different condition such as grinding, reflux, microwave and ultrasound irradiation. The obtained dihydroperimidines were characterized by spectroscopic and physical methods such as FT-IR, <sup>1</sup>H NMR and melting point. Short reaction times, high conversions, clean reaction profiles, simple work-up, availability and low cost of catalysts and absence of any hazardous organic solvents are some advantages of these protocols. Also, this heterogeneous acidic magnetic nano catalyst could be successfully reused at least for five runs without significant loss in its activity.

**How to cite this article**

Mazoochi A., Bamoniri A., Pourmousavi S.A. Synthesis of 2,3-dihydroperimidines in the Presence of Nano- $\gamma$ - $\text{Al}_2\text{O}_3/\text{BF}_n$  and Nano- $\gamma$ - $\text{Al}_2\text{O}_3/\text{BF}_n/\text{Fe}_3\text{O}_4$  as Catalysts under Different Conditions. J Nanostruct, 2021; 11(2): 554-567. DOI: 110.22052/JNS.2021.03.013

## INTRODUCTION

Nitrogen containing fused heterocyclic naphthalenes are good candidates for biological, agricultural and medicinal applications [1,2]. Perimidines exhibit a diverse range of biological properties, such as anti-fungal, antimicrobial, anti-ulcer, antimalarial, antioxidant and anti-tumor activities [3-8]. In the perimidine core the lone pair of nitrogen atoms participates in the  $\pi$ -system of the molecule which results in a transfer of electron density to naphthalene rings from the heterocyclic part and thus behaves as  $\pi$ -deficient as well as  $\pi$ -excessive system. They have been widely used

\* Corresponding Author Email: [bamoniri@kashanu.ac.ir](mailto:bamoniri@kashanu.ac.ir)

as coloring materials and dye intermediates for polymers, polyester fibers and more recently as source of a novel carbene ligand [9,10].

Synthesis of 2,3-dihydro-1H-perimidine comprises reaction of naphthalene-1,8-diamine with various carbonyl functionalities under acidic condition [11,12]. The most frequent approach used for the preparation of dihydroperimidine derivatives is the reaction of naphthalene-1,8-diamine with aldehydes.

Today, synthesis of organic compounds using solid acid catalysts is more and more attention due to the numerous advantages such as cost-

effectiveness, high catalytic activity, ease of product separation, recovery of the catalyst, repeated recycling potential and good stability [13-15]. Previously, the synthesis of dihydroperimidine derivatives was done using NaY zeolite [16], Anhyd. PhB(OH)<sub>2</sub> [17], Fe<sub>3</sub>O<sub>4</sub>@b-CD-ZrO [18], FePO<sub>4</sub> [19], Amberlyst 15 [20], HBOB [21],  $\gamma$ -Al<sub>2</sub>O<sub>3</sub>/SbCl<sub>5</sub> [22], Ytterbium(III) Triflate [23] and Fe<sub>3</sub>O<sub>4</sub>/SiO<sub>2</sub>/(CH<sub>2</sub>)<sub>3</sub>N<sup>+</sup>Me<sub>3</sub>Br<sub>3</sub><sup>-</sup> [24] as catalysts.

Alumina supported BF<sub>3</sub> is a mild solid lewis acid that promotes acidic catalyzed organic reactions. This catalyst does not need special precautions for preparation, handling, or storage. It can be stored at an ambient temperature for months without losing its catalytic activity.

Solid acid catalysts entitled nano- $\gamma$ -Al<sub>2</sub>O<sub>3</sub>/BF<sub>3</sub> and nano- $\gamma$ -Al<sub>2</sub>O<sub>3</sub>/BF<sub>n</sub>/Fe<sub>3</sub>O<sub>4</sub> were synthesized and characterized. Herein, they were successfully used for the synthesis of 2,3-dihydroperimidines.

## MATERIALS AND METHODS

### General

All compounds were purchased from Fluka and Merck chemical companies and used without any additional purification. A Bruker (DRX-400 Avance) NMR was used to record the <sup>1</sup>H NMR and <sup>13</sup>C NMR spectra. Fourier transform infrared (FT-IR) spectra were run on a Nicolet Magna 550 spectrometer. Vibrating-sample magnetometer (VSM) measurements were performed by using a vibrating sample magnetometer (Meghnatis Daghigh Kavir Co., Kashan, Iran). X ray diffraction (XRD) pattern using Philips Xpert MP diffractometer (Cu Ka, radiation,  $\lambda$  0.154056 nm) was achieved. Transmission electron microscope (TEM) was recorded on a Philips-CM 120-with LaB6 cathode instrument on an accelerating voltage of 120 kV. Thermal gravimetric analysis (TGA) was done with "STA 504" instrument. Field emission-scanning electron Microscopy (FE-SEM) was obtained on a Mira Tescan. Energy-dispersive x-ray spectroscopy (EDS) were measured by Phenom pro X. Brunauer-Emmett-Teller (BET) surface area analysis of catalysts were done with Micrometrics, Tristar II 3020 analyser. The ultrasonic irradiation experiments were carried out in a GD3200 probe ultrasonic device made by Bandelin Company with a frequency 20 - 120 kHz. The GE4020W microwave device, manufactured by Samsung, was used to perform irradiation.

### Preparation of nano- $\gamma$ -Al<sub>2</sub>O<sub>3</sub>

NaOH (600 ml, 1 M), was added drop-wise

to a slurry containing Al<sub>2</sub>(SO<sub>4</sub>)<sub>3</sub>.18H<sub>2</sub>O (66 g). The mixture was stirred at room temperature. The resulted suspension was filtered to obtain the white solid Al(OH)<sub>3</sub>. Then solid were washed with distilled water until no more sulfate ions were detected in the washings. Following the aging step, NaOH (100 ml, 1 M) was added to a beaker containing Al(OH)<sub>3</sub> (20 g) to produce NaAl(OH)<sub>4</sub>. Then PEG 4000 (0.3%) was added to solution and it was neutralized with HCl (0.1 M), to pH 8 until Al(OH)<sub>3</sub> produced again. The obtained precipitate filtered and washed with distilled water. The as-dried solid was calcined in the furnace at 800 °C for 3 hours through atmospheric air to produce nano- $\gamma$ -Al<sub>2</sub>O<sub>3</sub> powder [22].

### Preparation of nano- $\gamma$ -Al<sub>2</sub>O<sub>3</sub>/BF<sub>n</sub>

To a mixture of nano- $\gamma$ -Al<sub>2</sub>O<sub>3</sub> (5 g) and CH<sub>2</sub>Cl<sub>2</sub> (10 ml), Boron trifluoride etherate (10 ml) was added drop wise in the well ventilated hood. The resulting suspension was stirred for 15 minutes at room temperature, filtered, washed with CH<sub>2</sub>Cl<sub>2</sub>, and dried at room temperature [22].

### Preparation of nano- $\gamma$ -Al<sub>2</sub>O<sub>3</sub>/BF<sub>n</sub>/Fe<sub>3</sub>O<sub>4</sub>

For synthesis of nano- $\gamma$ -Al<sub>2</sub>O<sub>3</sub>/BF<sub>n</sub>/Fe<sub>3</sub>O<sub>4</sub>, to a suspension of 1 g of nano- $\gamma$ -Al<sub>2</sub>O<sub>3</sub>/BF<sub>n</sub> in 20 ml of dichloromethane, 1 g of Fe<sub>3</sub>O<sub>4</sub> nanoparticle was added and stirred in room temperature for 1 hours. Then, this suspension was filtered and dried in room temperature [13].

### General procedures for the preparation of 2,3-dihydroperimidines

#### Grinding method

naphthalene-1,8-diamine (1 mmol), aromatic aldehyde (1 mmol) and each of the nano catalysts (0.12 g and 0.06 g for nano- $\gamma$ -Al<sub>2</sub>O<sub>3</sub>/BF<sub>n</sub> and nano- $\gamma$ -Al<sub>2</sub>O<sub>3</sub>/BF<sub>n</sub>/Fe<sub>3</sub>O<sub>4</sub>, respectively) were grounded in a mortar with a pestle for a few minutes to obtain a homogeneous mixture, After completed conversion as indicated by TLC, 10 ml of ethanol was added and the heterogeneous catalyst was filtered. By adding crushed ice to filtrate, the pure product was obtained as white solid.

#### Reflux method

a mixture of naphthalene-1,8-diamine (1 mmol), aromatic aldehyde (1 mmol) and 0.12 g, 0.06 g of the catalysts mentioned (nano- $\gamma$ -Al<sub>2</sub>O<sub>3</sub>/BF<sub>n</sub>, nano- $\gamma$ -Al<sub>2</sub>O<sub>3</sub>/BF<sub>n</sub>/Fe<sub>3</sub>O<sub>4</sub>, respectively) in ethanol (10 mL) was heated under reflux (70 °C) for

the required time. After completion of the reaction which monitored by TLC, the reaction mixture was filtered to separate the nano catalysts. Also, the magnetic nano catalyst was separated by an external magnet. By adding cold water to residue, the product was appeared as a pure solid in high yield.

#### Microwave irradiation

In a 50 ml beaker, 1 mmol of naphthalene-1,8-diamine, 1 mmol of aromatic aldehyde and 0.06 g and 0.03 g of the catalysts were taken, respectively. Then 10 ml of ethanol as solvent was added to the reaction mixture. The reaction mixture was irradiated at 350W under microwave condition for specified time. The progress of the reaction was continuously monitored by checking TLC. After completion of reaction the reaction mixture was cooled down to room temperature. The solid crude product was slowly precipitated out of the reaction mixture. The crude product was recrystallized from hot ethanol to get pure product as solid powder.

#### Ultrasonic sono chemistry

In a 50 ml flask, a solution of naphthalene-1,8-diamine (1 mmol), aromatic aldehyde (1 mmol) in 10 ml of ethanol, the 0.03 g of each nano catalysts were sonicated at 80W, for appropriate times and monitored by TLC. After completed reaction, magnetic catalyst was separated by an external magnet. The mixture was dissolved in ethanol and poured into ice cold water. The resulting precipitate was filtered and recrystallized from ethanol.

All products in four methods were confirmed by comparing their melting points,  $^1\text{H}$  NMR and FT-IR spectral data with literature data.

#### Selected spectroscopic data

##### 2-(3-Nitrophenyl)-2,3-dihydro-1H-perimidine (Table 2, Entry 3)

Orange solid, M. F=  $\text{C}_{17}\text{H}_{13}\text{N}_3\text{O}_2$ , M. W= 291.23, M.P<sub>Obs.</sub> ( $^{\circ}\text{C}$ )= 170-173, M.P<sub>Rep.</sub> ( $^{\circ}\text{C}$ ) = 173 [25]. FT-IR [ $\bar{\nu}$  ( $\text{cm}^{-1}$ ) (KBr)]: 3343-3422 (NH), 3226 (=C-H), 2924 (C-H), 1526-1601 (C=C), 1261 (C-N), 1349 (N=O).  $^1\text{H}$  NMR (DMSO- $d_6$ , 400 MHz)  $\delta$  (ppm): 5.5 (1H, s, CH), 6.50 (2H, d,  $J=8$  Hz, CH), 7.00 (4H, d,  $J=8$  Hz, CH, NH), 7.15 (2H, t,  $J=8$  Hz, CH), 7.70 (1H, t,  $J=8$  Hz, CH), 8.02 (1H, d,  $J=8$  Hz, CH), 8.22 (1H, d,  $J=8$  Hz, CH), 8.42 (1H, s, CH<sub>3</sub>).

##### 2-(4-Methylphenyl)-2,3-dihydro-1H-perimidine (Table 2, Entry 5)

Yellow solid, M. F=  $\text{C}_{18}\text{H}_{16}\text{N}_2$ , M.W=260.2, M.P<sub>Obs.</sub> ( $^{\circ}\text{C}$ )= 158-161, M.P<sub>Rep.</sub> ( $^{\circ}\text{C}$ ) = 160-161 [26]. FT-IR [ $\bar{\nu}$  ( $\text{cm}^{-1}$ ) (KBr)]: 3367 (NH), 3039 (=C-H), 2919 (C-H aliphatic), 1484-1600 (C=C), 761-814.  $^1\text{H}$  NMR (DMSO- $d_6$ , 400 MHz)  $\delta$  (ppm): 2.50 (3H, s, CH<sub>3</sub>), 5.3 (1H, s, CH), 6.47 (2H, d,  $J=8$  Hz, CH), 6.7 (2H, s, NH), 6.96 (2H, d,  $J=8$  Hz, CH), 7.12 (2H, t,  $J=8$  Hz, CH), 7.22 (2H, d,  $J=8$  Hz, CH), 7.46 (2H, d,  $J=8$  Hz, CH).

##### 2-(4-Chlorophenyl)-2,3-dihydro-1H-perimidine (Table 2, Entry 6)

Gray Solid, M. F=  $\text{C}_{17}\text{H}_{13}\text{N}_2\text{Cl}$ , M. W= 280.64, M.P<sub>Obs.</sub> ( $^{\circ}\text{C}$ )= 171-173, M.P<sub>Rep.</sub> ( $^{\circ}\text{C}$ ) = 172-174 [26]. FT-IR [ $\bar{\nu}$  ( $\text{cm}^{-1}$ ) (KBr)]: 3387 (NH), 3034 (=C-H), 2797 (C-H), 1483-1599 (C=C), 1256 (C-N), 1087.17 (C-Cl), 758-814.  $^1\text{H}$  NMR (DMSO- $d_6$ , 400 MHz)  $\delta$  (ppm): 5.36 (1H, s, CH), 6.46 (2H, d,  $J=8$  Hz, CH), 6.8 (2H, s, NH), 6.97 (2H, d,  $J=8$  Hz, CH), 7.14 (2H, t,  $J=8$  Hz, CH), 7.46 (2H, d,  $J=8$  Hz, CH), 7.60 (2H, d,  $J=8$  Hz, CH).

##### 2-(2,4-Dichlorophenyl)-2,3-dihydro-1H-perimidine (Table 2, Entry 7)

Cream solid, M. F=  $\text{C}_{17}\text{H}_{12}\text{N}_2\text{Cl}_2$ , M. W= 315.19, M.P<sub>Obs.</sub> ( $^{\circ}\text{C}$ )= 159-161, M.P<sub>Rep.</sub> ( $^{\circ}\text{C}$ ) = 158-160 [26]. FT-IR [ $\bar{\nu}$  ( $\text{cm}^{-1}$ ) (KBr)]: 3238-3417 (NH), 3043 (=C-H), 2851-2923 (C-H), 1600 (C=C), 1264.18 (C-N), 1045.82 (C-Cl).  $^1\text{H}$  NMR (DMSO- $d_6$ , 400 MHz)  $\delta$  (ppm): 5.7 (1H, s, CH), 6.50 (2H, d,  $J=8$  Hz, CH), 6.70 (2H, s, NH), 7.02 (2H, d,  $J=8$  Hz, CH), 7.16 (2H, t,  $J=8$  Hz, CH), 7.50 (1H, d,  $J=8$  Hz, CH), 7.69 (2H, t,  $J=8$  Hz, CH).

##### 2-(3-Hydroxyphenyl)-2,3-dihydro-1H-perimidine (Table 2, Entry 10)

White solid, M. F=  $\text{C}_{17}\text{H}_{14}\text{N}_2\text{O}$ , M. W=262.19, M.P<sub>Obs.</sub> ( $^{\circ}\text{C}$ )= 183-187, M.P<sub>Rep.</sub> ( $^{\circ}\text{C}$ ) = 185-188 [25]. FT-IR [ $\bar{\nu}$  ( $\text{cm}^{-1}$ ) (KBr)]: 3427 (OH), 3233 (NH), 2923 (=C-H), 2852 (C-H), 1602. (C=C), 1335 (C-N), 1123.47 (C-O).  $^1\text{H}$  NMR (DMSO- $d_6$ , 400 MHz)  $\delta$  (ppm): 5.2 (1H, s, CH), 6.46 (2H, d,  $J=8$  Hz, CH), 6.7 (2H, s, NH exchange with D<sub>2</sub>O), 6.75, (1H, d,  $J=8$  Hz), 6.95 (2H, d,  $J=8$  Hz), 6.99 (2H, d,  $J=8$  Hz, CH), 7.12 (2H, t,  $J=8$  Hz, CH), 7.19 (1H, t,  $J=8$  Hz), 9.4 (1H, s, OH, exchange with D<sub>2</sub>O).

##### 2-(2-Methoxyphenyl)-2,3-dihydro-1H-perimidine (Table 2, Entry 12)

White solid, M. F=C<sub>17</sub>H<sub>16</sub>N<sub>2</sub>O, M. W=264.19, M.P<sub>Obs.</sub> (° C) = 122-126, M.P<sub>Rep.</sub> (° C) = 124-127 [25]. FT-IR [ $\bar{\nu}$  (cm<sup>-1</sup>) (KBr)]: 3380 (NH), 3046 (=C-H), 2925 (C-H), 1596 (C=C), 1239 (C-N), 1025 (C-O). <sup>1</sup>H NMR (DMSO-d<sub>6</sub>, 400 MHz)  $\delta$  (ppm): 3.86 (3H, s, CH<sub>3</sub>), 5.52 (1H, s, CH), 6.46 (2H, d, J=8 Hz, CH), 6.56 (2H, s, NH), 6.97 (3H, d, J=8 Hz, CH), 7.08 (1H, d, J=8 Hz), 7.12 (2H, t, J=8 Hz, CH), 7.33 (1H, t, J=8 Hz), 7.55 (1H, d, J=8 Hz).

*2-(3,4-Dimethoxyphenyl)-2,3-dihydro-1H-perimidine (Table 2, Entry 13)*

Yellow Solid, M. F= C<sub>19</sub>H<sub>18</sub>N<sub>2</sub>O<sub>2</sub>, M. W= 306.17, M. P<sub>Obs.</sub> (° C) = 205-207, M. P<sub>Rep.</sub> (° C) = 205-208 [11]. FT-IR [ $\bar{\nu}$  (cm<sup>-1</sup>) (KBr)]: 1024 (C-O), 1263 (C-N), 1379 (CH<sub>3</sub> bend), 1599, 1460 (C=C), 2998 (C-H), 3350 (NH). <sup>1</sup>H NMR (DMSO-d<sub>6</sub>, 400 MHz)  $\delta$  (ppm): 3.79 (3H, s, CH<sub>3</sub>), 3.76 (3H, s, CH<sub>3</sub>), 5.27 (1H, s, CH), 6.47 (2H, d, J=8 Hz, CH), 6.66 (1H, s, NH exchange with D<sub>2</sub>O), 6.97 (3H, d, J=8 Hz, CH), 7.12 (4H, d, J=8. Hz, CH), 7.20 (1H, s, NH exchange with D<sub>2</sub>O).

*2-(3-Ethoxy, 4-hydroxyphenyl)-2,3-dihydro-1H-perimidine (Table 2, Entry 15)*

Pink solid, M. F=C<sub>19</sub>H<sub>18</sub>N<sub>2</sub>O<sub>2</sub>, M. W=306.21, M.P<sub>Obs.</sub> (° C) = 190-191. FT-IR [ $\bar{\nu}$ (cm<sup>-1</sup>) (KBr)]: 3464 (OH), 3307-3336 (NH), 3060.07 (=C-H), 2975 (C-H), 1522-1598 (C=C), 1256 (C-N), 1038 (C-O) .<sup>1</sup>H NMR (DMSO-d<sub>6</sub>, 400 MHz)  $\delta$  (ppm):1.34 (3H, t, J=6 Hz,

CH<sub>3</sub>), 4.02 (2H, q, J=6 Hz, CH<sub>2</sub>), 5.22 (1H, s, CH), 6.45 (2H, d, J=8 Hz, CH), 6.60 (2H, s, NH exchange with D<sub>2</sub>O), 6.80 (1H, d, J=8 Hz, CH), 6.96 (3H, t, J=8 Hz, CH), 7.12 (3H, t, J=8 Hz, CH), 9.1 (1H, s, OH, exchange with D<sub>2</sub>O).

## RESULTS AND DISCUSSION

In continuation of our research on the applications of solid acids in organic synthesis, we have investigated nano- $\gamma$ -Al<sub>2</sub>O<sub>3</sub>/BF<sub>n</sub> and nano- $\gamma$ -Al<sub>2</sub>O<sub>3</sub>/BF<sub>n</sub>/Fe<sub>3</sub>O<sub>4</sub> efficiency in the synthesis of 2,3-dihydroperimidines by different conditions. For identification of the structure of nano- $\gamma$ -Al<sub>2</sub>O<sub>3</sub>/BF<sub>n</sub>, we have studied FT-IR (ATR) spectra of nano- $\gamma$ -Al<sub>2</sub>O<sub>3</sub> and nano- $\gamma$ -Al<sub>2</sub>O<sub>3</sub>/BF<sub>n</sub> (Fig. 1). In nano- $\gamma$ -Al<sub>2</sub>O<sub>3</sub> FT-IR spectrum, strong bands at 1742, 1370 and 1216 cm<sup>-1</sup> were observed. In nano- $\gamma$ -Al<sub>2</sub>O<sub>3</sub>/BF<sub>n</sub>, in addition to the above mentioned bands, three bands also appeared at 1627, 1410 and 1071 cm<sup>-1</sup>. The peaks at 1410 and 1071 cm<sup>-1</sup> verify the B-O and Al-O-B bonds on nano- $\gamma$ -Al<sub>2</sub>O<sub>3</sub>/BF<sub>n</sub> respectively.

The FESEM image of nano- $\gamma$ -Al<sub>2</sub>O<sub>3</sub>/BF<sub>n</sub> is shown in Fig. 2.

EDS of nano- $\gamma$ -Al<sub>2</sub>O<sub>3</sub>/BF<sub>n</sub> was measured (Fig. 3). According to this data, the weight percentage of O, Al and F are 42.8, 34.9 and 22.3, respectively. The amount of boron in nano- $\gamma$ -Al<sub>2</sub>O<sub>3</sub>/BF<sub>n</sub> was determined. For this purpose, a mixture of nano-

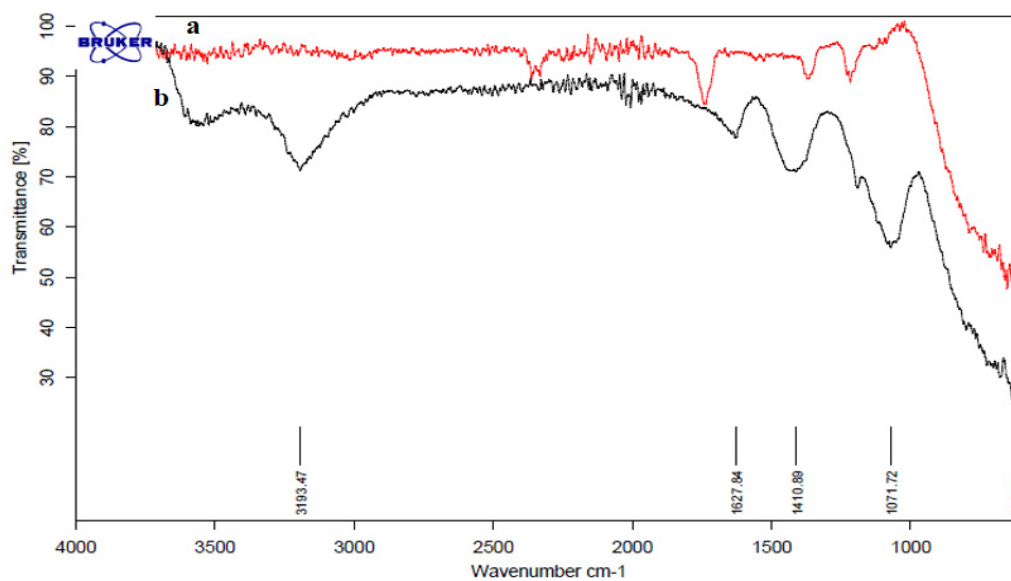


Fig. 1. FT-IR spectra of: (a) nano-Al<sub>2</sub>O<sub>3</sub>, (b) nano- $\gamma$ -Al<sub>2</sub>O<sub>3</sub>/BF<sub>n</sub>

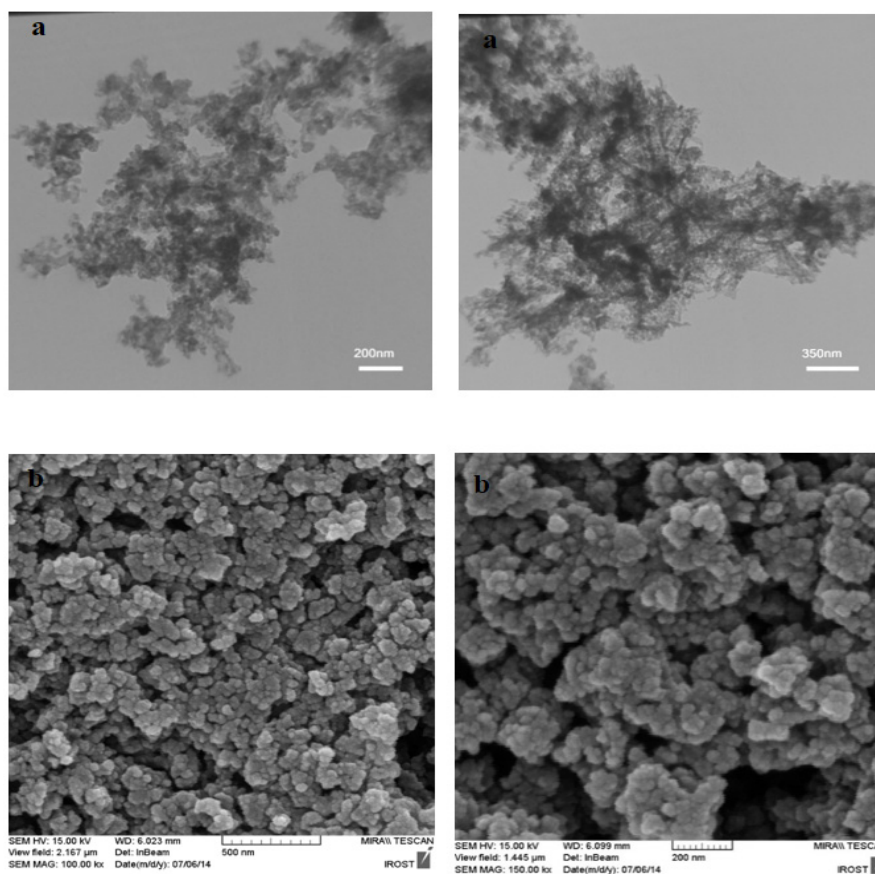


Fig. 2. TEM (a) and FESEM (b) images of nano- $\gamma$ -Al<sub>2</sub>O<sub>3</sub>/BF<sub>n</sub>

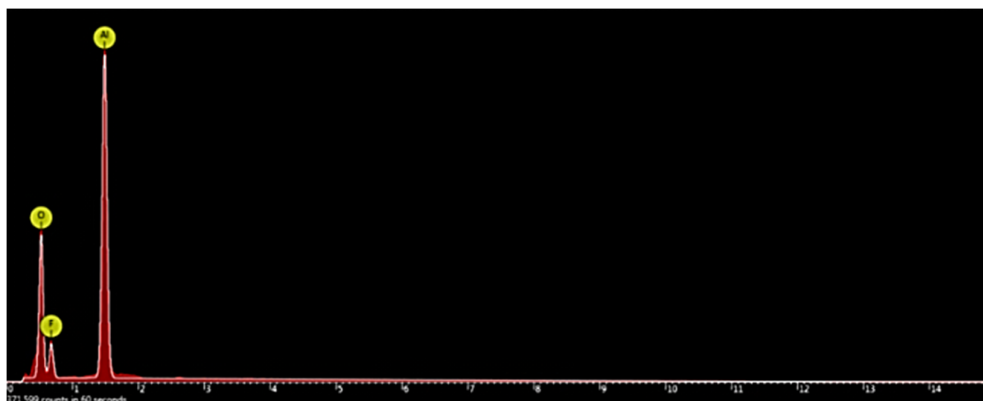


Fig. 3. EDS analysis diagram of nano- $\gamma$ -Al<sub>2</sub>O<sub>3</sub>/BF<sub>n</sub>

$\gamma$ -Al<sub>2</sub>O<sub>3</sub>/BF<sub>n</sub> (0.1 g) and water (50 ml) was stirred and boiled for 20 minutes. Then, the mixture was cooled and titrated with 23 ml of standard NaOH (0.009 N) in the presence of phenolphthalein. The boron amount in catalyst was found to be 2.1 meq.g<sup>-1</sup>. In this process, the attached boron

in nano- $\gamma$ -Al<sub>2</sub>O<sub>3</sub>/BF<sub>n</sub> was reacted with water, captured OH from water to produce B(OH)<sub>4</sub><sup>-</sup> and H<sup>+</sup>. The amount of H<sup>+</sup> that evaluated with titration is equal boron.

XRD pattern of nano- $\gamma$ -Al<sub>2</sub>O<sub>3</sub>/BF<sub>n</sub> is shown in Fig. 4. According to XRD pattern of catalyst, two

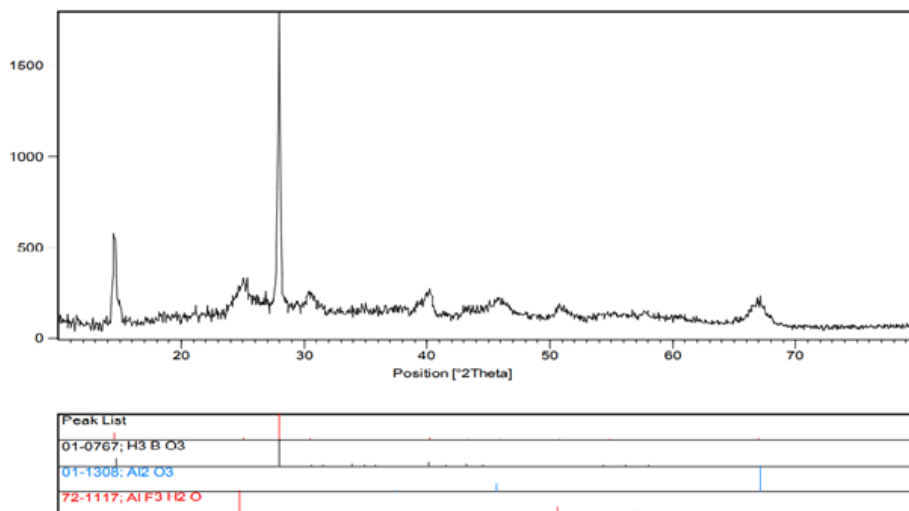


Fig. 4. XRD patterns of nano- $\gamma$ -Al<sub>2</sub>O<sub>3</sub>/BF<sub>n</sub>

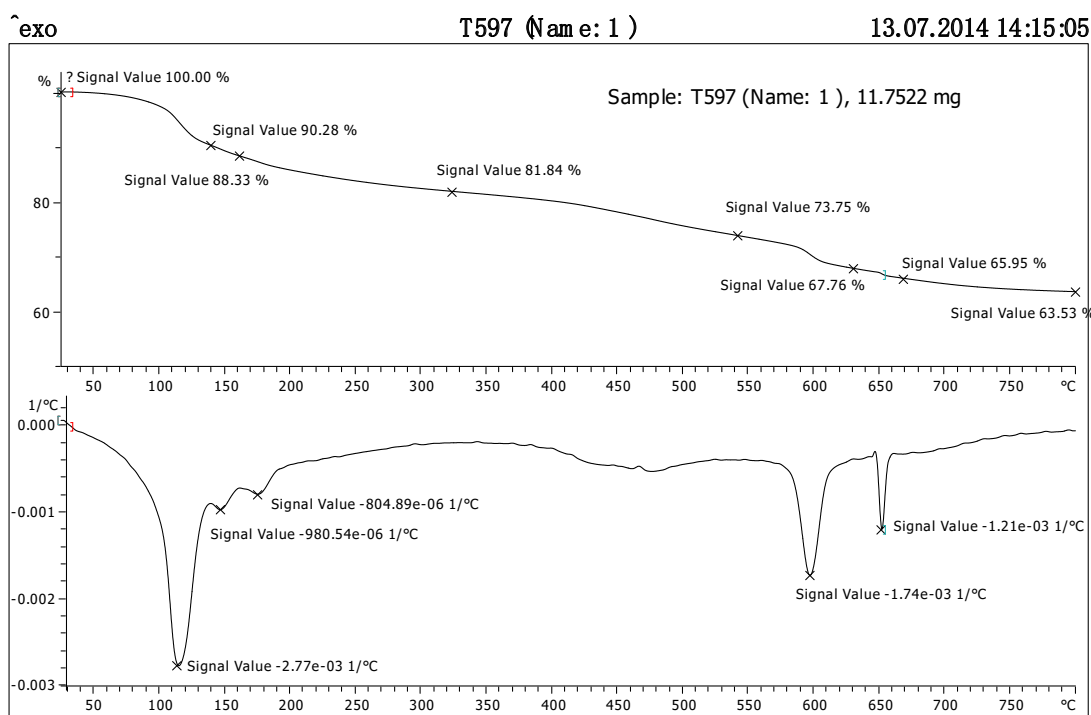


Fig. 5. Thermal gravimetric analysis (TG-DTA) pattern of nano- $\gamma$ -Al<sub>2</sub>O<sub>3</sub>/BF<sub>n</sub>

signals at  $2\theta$  equal to 14.57 and 27.96 with FWHM equal to 0.2952 and 0.1771 respectively, is similar to HBO<sub>3</sub> with B-O bonds. The signals at  $2\theta$  equal to 25.09, 45.91 and 66.99 are shown  $\gamma$ -Al<sub>2</sub>O<sub>3</sub> structure.

TGA pattern of nano- $\gamma$ -Al<sub>2</sub>O<sub>3</sub>/BF<sub>n</sub> was detected from 50 to 800 °C (Fig. 5). The catalyst is stable until 100 °C and only 10% of its weight was reduced in

115 °C. This initial reducing mass (10%) of catalyst is related to removal of catalyst moisture. By heating of catalyst between 600 °C to 660 °C, the reducing amount of its weight is 6% *via* cleavage of B-F bonds. According to TGA diagram of nano- $\gamma$ -Al<sub>2</sub>O<sub>3</sub>/BF<sub>n</sub>, this catalyst is stable until 100°C.

The FT-IR spectra of nano- $\gamma$ -Al<sub>2</sub>O<sub>3</sub>/BF<sub>n</sub>/Fe<sub>3</sub>O<sub>4</sub> display significant peaks at 1095 and 796 cm<sup>-1</sup>

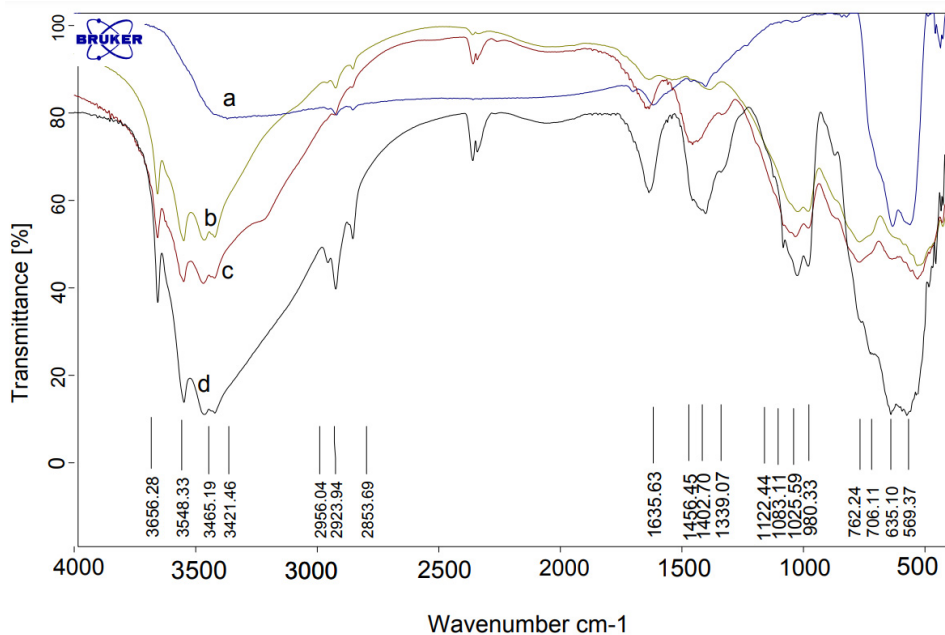


Fig. 6. FT-IR spectra of: (a)  $Fe_3O_4$ , (b) nano- $\gamma-Al_2O_3$ , (c) nano- $\gamma-Al_2O_3/BF_n$ , (d) nano- $\gamma-Al_2O_3/BF_n/Fe_3O_4$

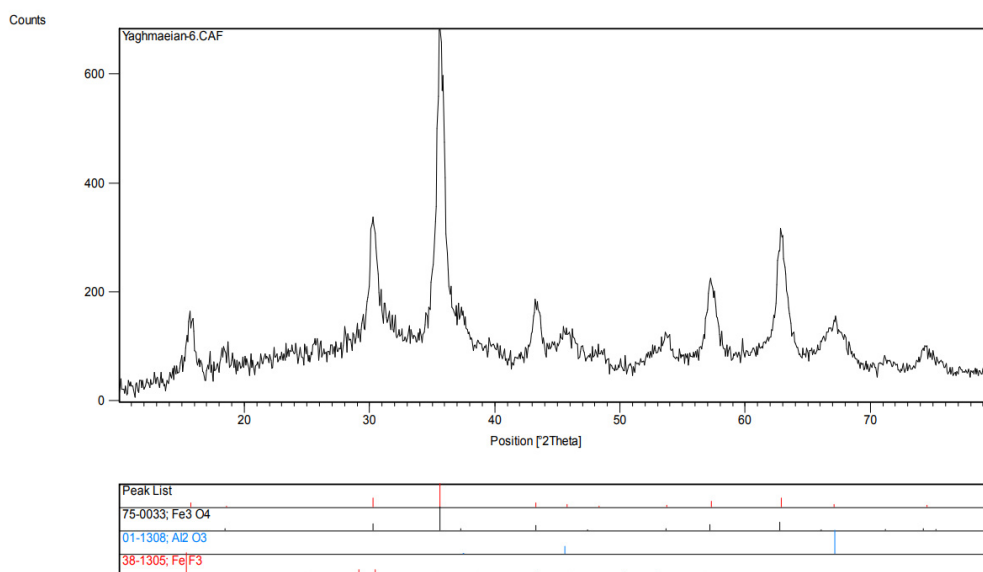


Fig. 7. X-ray diffraction (XRD) pattern of nano- $\gamma-Al_2O_3/BF_n/Fe_3O_4$

corresponding to symmetrical and asymmetrical vibrations of Al-O-Al, respectively (Fig. 6). Weak band at  $459\text{ cm}^{-1}$  regarding to the Al-O-Fe stretching vibrations of the  $\gamma-Al_2O_3/Fe_3O_4$ . These results show that  $Fe_3O_4$  is immobilized on the surface of  $Al_2O_3$ . The successful covalent bonding of  $BF_3$  on the surface of  $Al_2O_3$  was confirmed by the band available at  $1623\text{ cm}^{-1}$ , which originates from the absorption of O- $BF_3$ .

XRD pattern of the nano- $\gamma-Al_2O_3/BF_3$  (A),  $Fe_3O_4$  (B) and  $\gamma-Al_2O_3/BF_n/Fe_3O_4$  (C) is characterized in Fig. 7. The signals at  $2\theta$  equal to 40 (c) and 67 (d) display nano- $\gamma-Al_2O_3$  structure. Two additional signals at  $2\theta$  equal to 15 (a) and 28 (b) are exposed the presence of bonded  $BF_3$  to nano- $\gamma-Al_2O_3$ , respectively. According to Debye Scherrer equation ( $\tau = K\lambda/\beta\cos\theta$ ) the crystallite size equal to 6.5 nm ( $\beta = 0.5$ ,  $\theta = 11$ ,  $K = 0.94$ ,  $\lambda = 0.154\text{ nm}$ )

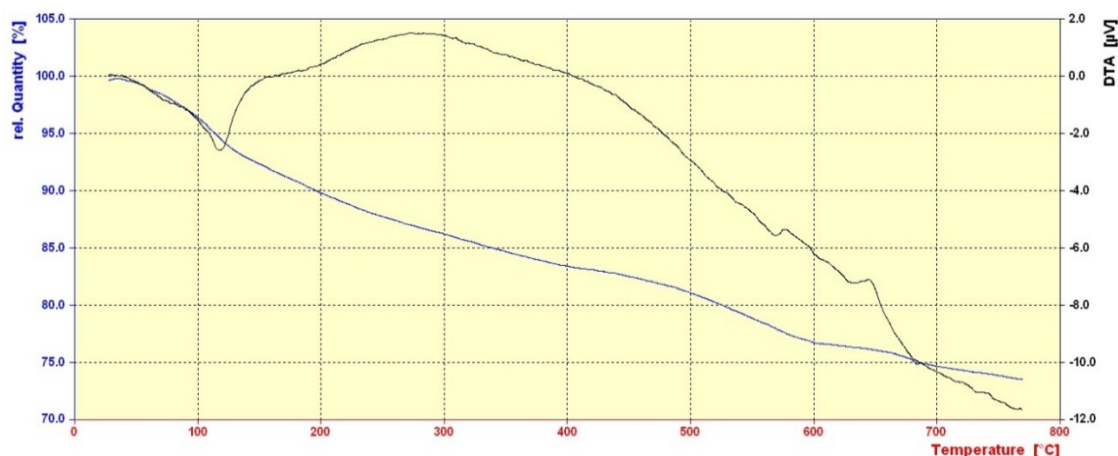


Fig. 8. Thermal gravimetric analysis (TG-DTA) pattern of nano- $\gamma$ - $\text{Al}_2\text{O}_3/\text{BF}_n/\text{Fe}_3\text{O}_4$

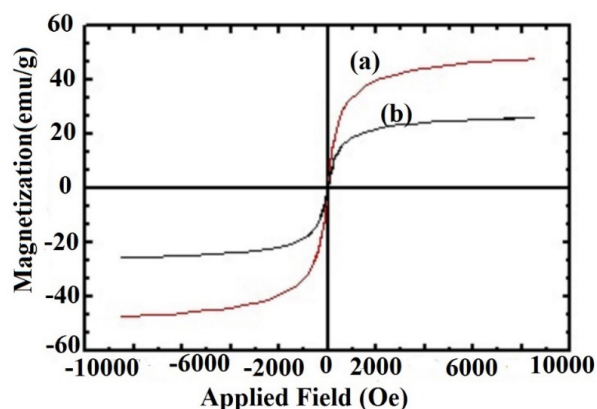


Fig. 9. VSM images of (a)  $\text{Fe}_3\text{O}_4$  and (b) nano- $\gamma$ - $\text{Al}_2\text{O}_3/\text{BF}_n/\text{Fe}_3\text{O}_4$

has been detected. In the spectra of  $\text{Fe}_3\text{O}_4$  nano particles, the wide band at  $1627$  and  $3446\text{ cm}^{-1}$  are corresponding to the surface adsorbed water and hydroxyl groups of  $\text{Fe}_3\text{O}_4$  nano particles, while the peaks at  $459$  and  $598\text{ cm}^{-1}$  are respectively corresponding to the octahedral bending and tetrahedral stretching vibration of the Fe–O functional group and the peak at  $630\text{ cm}^{-1}$  approves the existence of  $\text{Fe}_3\text{O}_4$  structure.

TG-DTA pattern of  $\gamma\text{-Al}_2\text{O}_3/\text{BF}_n/\text{Fe}_3\text{O}_4$  was identified using heating from  $0\text{ }^\circ\text{C}$  to  $800\text{ }^\circ\text{C}$  (Fig. 8). TGA curve of the catalyst advises a preliminary weight loss of  $0\%$  below  $200\text{ }^\circ\text{C}$ , owing to the physically adsorbed water on the  $\text{Al}_2\text{O}_3$ . According to the TGA diagram of nano- $\gamma\text{-Al}_2\text{O}_3/\text{BF}_n/\text{Fe}_3\text{O}_4$ , it was shown that this catalyst is suitable for the catalysis of organic reactions up to  $100\text{ }^\circ\text{C}$ .

The magnetization curve of magnetite nanoparticles is shown in Fig. 9 at room

temperature by VSM. Within the VSM magnetization curves of  $\text{Fe}_3\text{O}_4$  and  $\gamma\text{-Al}_2\text{O}_3/\text{BF}_n/\text{Fe}_3\text{O}_4$  nanoparticles, there is a lack of hysteresis, and the remanence and coercivity is negligible, which reveals the superparamagnetism of these nanomaterials. The saturation magnetization value of nano- $\gamma\text{-Al}_2\text{O}_3/\text{BF}_n/\text{Fe}_3\text{O}_4$  ( $28.3\text{ emu g}^{-1}$ ) is below that of  $\text{Fe}_3\text{O}_4$  ( $62.3\text{ emu g}^{-1}$ ) because of the existence of a nonmagnetic  $\text{Al}_2\text{O}_3/\text{BF}_n$  coating.

The specific surface area of catalyst was measured *via* BET theory. The BET surface area is assigned as  $131.73\text{ m}^2\text{ g}^{-1}$ . The Nitrogen adsorption isotherm of catalyst is described in Fig. 10.

The FE-SEM images of the nano- $\gamma\text{-Al}_2\text{O}_3/\text{BF}_n/\text{Fe}_3\text{O}_4$  nanoparticles are shown in Fig. 11. By using SEM, the particle size and morphology of the nano- $\gamma\text{-Al}_2\text{O}_3/\text{BF}_n/\text{Fe}_3\text{O}_4$  was examined. An irregular spherical shape has been displayed for nanoparticles below  $5\text{ }\mu\text{m}$ . TEM measurement was



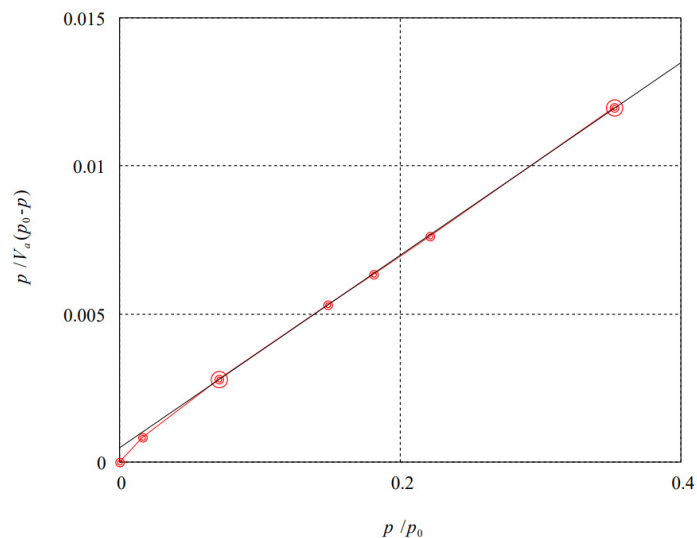


Fig. 10. Nitrogen adsorption of nano- $\gamma$ -Al<sub>2</sub>O<sub>3</sub>/BF<sub>n</sub>/Fe<sub>3</sub>O<sub>4</sub>

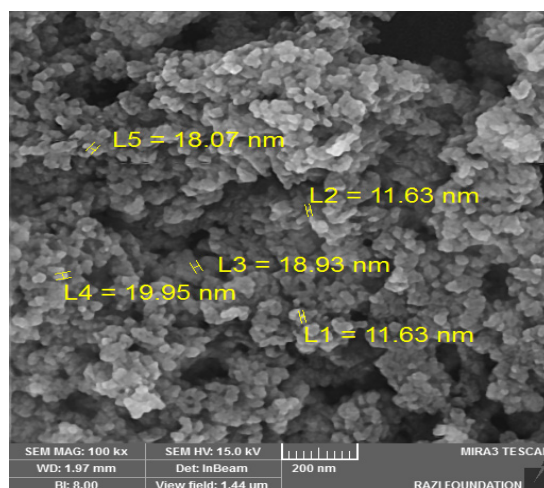


Fig. 11. FESEM image of nano- $\gamma$ -Al<sub>2</sub>O<sub>3</sub>/BF<sub>n</sub>/Fe<sub>3</sub>O<sub>4</sub>

used to confirm the structure of nano- $\gamma$ -Al<sub>2</sub>O<sub>3</sub>/BF<sub>n</sub>/Fe<sub>3</sub>O<sub>4</sub> as nano catalyst in Fig. 12. The TEM image of nano- $\gamma$ -Al<sub>2</sub>O<sub>3</sub>/BF<sub>n</sub>/Fe<sub>3</sub>O<sub>4</sub> displays an integrated nano- $\gamma$ -Al<sub>2</sub>O<sub>3</sub>/BF<sub>n</sub> coating gathered on the exterior of Fe<sub>3</sub>O<sub>4</sub>, demonstrating the core/shell structure of the catalyst.

After characterization of two catalysts, we have investigated catalytic activity of these catalysts for the synthesis of 2,3- dihydroperimidine derivatives. For optimization of the reaction reservations, 1,8-diaminonaphthalene (1mmol), and 4-chlorobenzaldehyde (1mmol) in the presence of nano- $\gamma$ -Al<sub>2</sub>O<sub>3</sub>/BF<sub>n</sub> and nano- $\gamma$ -Al<sub>2</sub>O<sub>3</sub>/

BF<sub>n</sub>/Fe<sub>3</sub>O<sub>4</sub> under various conditions were used as model reactants (Table 1). The best resultant based on the amount of catalysts, yield and time of the reaction were afforded with 0.12, 0.12, 0.06 and 0.03 g of nano- $\gamma$ -Al<sub>2</sub>O<sub>3</sub>/BF<sub>n</sub> and 0.06, 0.06, 0.03 and 0.03 g of nano- $\gamma$ -Al<sub>2</sub>O<sub>3</sub>/BF<sub>n</sub>/Fe<sub>3</sub>O<sub>4</sub> for grinding, reflux, microwave and ultrasonic methods, respectively. Also, Table 1, shows the performance of our nano-catalysts in the preparation of 2,3-dihydroperimidines contrast to that of other reported methods.

Using the optimized reaction provisions, the reactions of various substituted aromatic

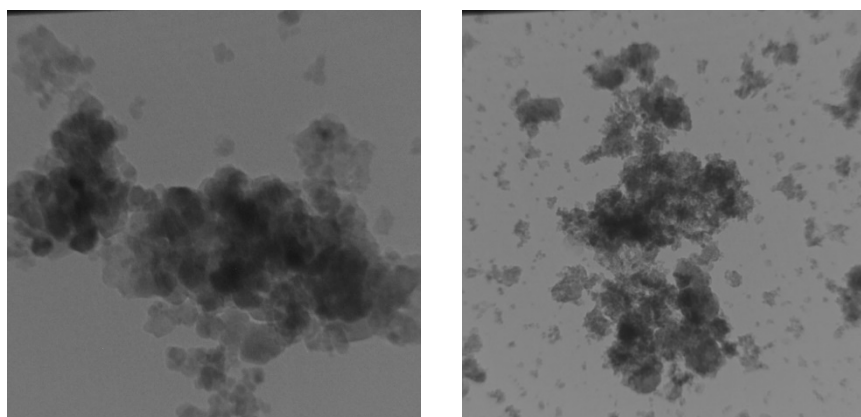
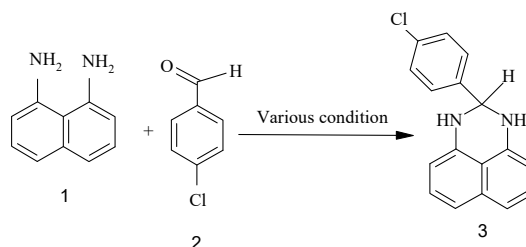


Fig. 12. TEM images of nano- $\gamma$ -Al<sub>2</sub>O<sub>3</sub>/BF<sub>3</sub>/Fe<sub>3</sub>O<sub>4</sub>

Table 1. Condensation of 4-chlorobenzaldehyde and 1,8-diaminonaphthalene under various conditions <sup>a</sup>



Entry	Catalyst	Methods				Ref.
		Grinding S. F./ R.T	Reflux EtOH/ 70 °C	Microwave EtOH/ 350 Watt	Ultrasonic EtOH/ 80 Watt	
		Catalyst / Time (min)/ Yield <sup>b</sup> (%)	Catalyst / Time (min)/ Yield <sup>b</sup> (%)	Catalyst / Time (min)/ Yield <sup>b</sup> (%)	Catalyst / Time (min)/ Yield <sup>b</sup> (%)	
1	Phenyl boronic acid	0.2 mmol/ 75/ 95	-	-	-	14
2	Fe <sub>3</sub> O <sub>4</sub> @ $\beta$ -CD-ZrO <sub>2</sub>	0.04 g/ 20/ 85	-	-	-	15
3	Catalyst-free, on water protocol	-/30/ 98	-	-	-	4
4	FePO <sub>4</sub>	10 mol%/ 420/ 90	-	-	-	6
5	NaY Zeolite	0.20 g /2700/ 47%	-	-	-	13
6	Amberlyst 15	20%w/w/ 135/ 97	-	-	-	17
7	HBOB	10 mol%/ 60/ 95	-	-	-	18
8	Ytterbium (III) Triflate	3 mmol%/ 180/ 91	-	-	-	20
9	$\gamma$ -Al <sub>2</sub> O <sub>3</sub> /SbCl <sub>5</sub>	0.16 g/ 15/ 93	-	-	-	19
10	nano- $\gamma$ -Al <sub>2</sub> O <sub>3</sub> /BF <sub>3</sub>	0.03 g/ 20/ 80	0.03 g/ 30/ 80	0.03 g/ 4/ 82	0.03 g/ 3/ 95	This Work
11	nano- $\gamma$ -Al <sub>2</sub> O <sub>3</sub> /BF <sub>3</sub>	0.06 g/ 25/ 82	0.06 g/ 25/ 85	0.06 g/ 3/ 95	0.06 g/ 4/ 90	This Work
12	nano- $\gamma$ -Al <sub>2</sub> O <sub>3</sub> /BF <sub>3</sub>	0.12 g / 15/ 94	0.12 g / 20/ 94	0.12 g/ 3/ 86	0.12 g/ 4/ 88	This Work
13	nano- $\gamma$ -Al <sub>2</sub> O <sub>3</sub> /BF <sub>3</sub> /Fe <sub>3</sub> O <sub>4</sub>	0.03 g/ 20/ 80	0.03 g/ 25/ 80	0.03 g / 3/ 97	0.03 g/ 3/ 96	This Work
14	nano- $\gamma$ -Al <sub>2</sub> O <sub>3</sub> /BF <sub>3</sub> /Fe <sub>3</sub> O <sub>4</sub>	0.06 g/ 15/ 96	0.06 g/ 15/ 96	0.06 g / 4/ 90	0.06 g/ 3/ 92	This Work
15	nano- $\gamma$ -Al <sub>2</sub> O <sub>3</sub> /BF <sub>3</sub> /Fe <sub>3</sub> O <sub>4</sub>	0.12 g/ 25/ 90	0.12 g/ 20/ 90	0.12 g/ 3/ 88	0.12 g / 4/ 89	This Work

<sup>a</sup>1,8-Diaminonaphthalene (1 mmol), and 4-chlorobenzaldehyde (1 mmol) were used.

<sup>b</sup> Isolated yield.

aldehydes with naphthalene-1,8- diamine in the presence of two catalyst were studied (Fig. 13, Tables 2, 3). As displayed in Tables, a number of aromatic aldehydes bearing electron withdrawing groups and electron-donating groups were further subjected to reaction. In general, with

electron-drawing substituents in the aromatic benzaldehydes, increased yields of products were generated, whereas the affect is reversed with electron donating substituents. However, the variations in the yields were little.

The proposed mechanism for the synthesis of

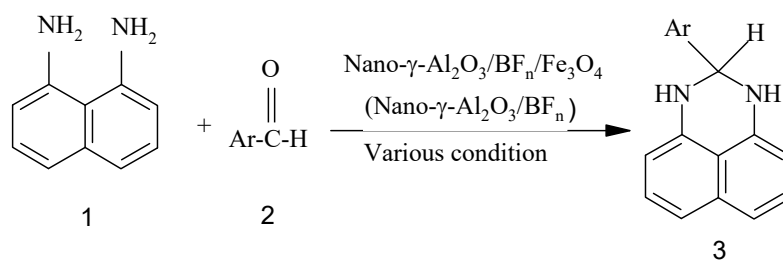
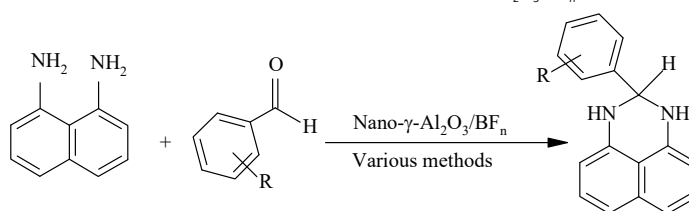


Fig. 13. Synthesis of 2,3-dihydroperimidines

Table 2. Synthesis of 2-substituted perimidines using nano- $\gamma$ -Al<sub>2</sub>O<sub>3</sub>/BF<sub>n</sub> catalyst<sup>a</sup>



Entry	R	Product	Methods			
			Grinding S. F./R.T	Reflux EtOH/70 °C	Microwave EtOH/350 Watt	Ultrasonic EtOH/80 Watt
			Time (min)/ Yield <sup>b</sup> (%)	Time (min)/ Yield <sup>b</sup> (%)	Time (min)/ Yield <sup>b</sup> (%)	Time (min)/ Yield <sup>b</sup> (%)
1	H	3a	30/72	25/75	4/79	3/78
2	2-NO <sub>2</sub>	3b	20/82	20/84	4/88	3/92
3	3-NO <sub>2</sub>	3c	25/80	20/82	4/92	3/95
4	4-COOH	3d	35/79	40/82	5/84	4/87
5	4-Me	3e	35/76	40/80	6/86	5/86
6	4-Cl	3f	40/78	35/82	6/86	4/86
7	2,4-Cl	3g	30/80	35/78	6/82	5/85
8	2,6-Cl	3h	30/78	35/80	5/82	5/86
9	2-OH	3i	35/76	35/78	5/81	5/86
10	3-OH	3j	35/75	35/76	4/80	4/85
11	2,4-OH	3k	40/70	35/70	6/78	5/80
12	2-OMe	3l	40/71	40/70	5/71	5/79
13	3,4-OMe	3m	45/69	40/70	6/72	5/74
14	2-OH,3-OMe	3n	45/69	40/69	6/73	5/79
15	4-OH, 3-OEt	3o	45/70	40/70	5/70	5/79

<sup>a</sup> 1,8-Diaminonaphthalene (1 mmol), aldehyde (1 mmol) and nano- $\gamma$ -Al<sub>2</sub>O<sub>3</sub>/BF<sub>3</sub> (0.12, 0.12, 0.06, and 0.03g for grinding, reflux, microwave and ultrasonic methods, respectively) were used.

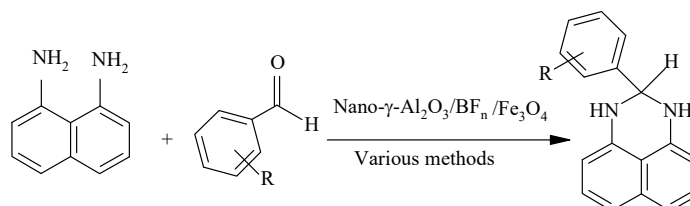
<sup>b</sup> Isolated yield.

2,3-dihydroperimidines is similar for both catalysts and is shown in Fig. 14. BF<sub>3</sub> in each of the catalysts as a Lewis acid activates the carbonyl group in aromatic aldehydes. As you can see, the first step in this mechanism is the formation of a complex between the empty boron orbital and the oxygen electron pair in the aldehyde. At this point, the C = O bond is activated for a nucleophilic attack. In the next step, the 1,8-diamino-naphthalene molecule attacks the carbonyl group to produce the intermediate (I), and the displacement of a hydrogen group and the loss of a water molecule

give intermediate (III), then an intramolecular cyclization and the recapture of a hydrogen molecule, the desired 2,3-dihydropyrimidine is obtained.

The reusability of the catalysts is one of the most important benefits that make them useful for commercial applications. The nano- $\gamma$ -Al<sub>2</sub>O<sub>3</sub>/BF<sub>n</sub>/Fe<sub>3</sub>O<sub>4</sub> catalyst can be easily separated by magnet and reused after washing with CHCl<sub>3</sub> and drying at 50°C under vacuum for 1 h. The separated magnetic catalyst was reused in the mentioned reaction) 1,8-diaminonaphthalene

Table 3. Synthesis of 2-substituted perimidines using nano- $\gamma$ -Al<sub>2</sub>O<sub>3</sub>/BF<sub>n</sub>/ Fe<sub>3</sub>O<sub>4</sub> catalyst<sup>a</sup>



Entry	R	Product	Methods			
			Grinding	Reflux	Microwave	Ultrasonic
			S. F./R.T	EtOH/70 °C	EtOH/350 Watt	EtOH/80 Watt
			Time (min)/ Yield <sup>b</sup> (%)	Time (min)/ Yield <sup>b</sup> (%)	Time (min)/ Yield <sup>b</sup> (%)	Time (min)/ Yield <sup>b</sup> (%)
1	H	3a	25/74	25/79	4/84	3/83
2	2-NO <sub>2</sub>	3b	20/84	20/85	4/90	3/95
3	3-NO <sub>2</sub>	3c	20/82	25/84	4/94	3/96
4	4-COOH	3d	30/79	30/82	4/84	4/87
5	4-Me	3e	30/75	30/80	6/86	5/86
6	4-Cl	3f	25/79	30/83	5/86	4/87
7	2,4-Cl	3g	30/82	35/79	6/85	4/85
8	2,6-Cl	3h	30/80	35/82	5/84	5/86
9	2-OH	3i	32/79	40/79	5/83	4/87
10	3-OH	3j	35/79	40/79	4/82	4/86
11	2,4-OH	3k	30/75	35/75	6/80	5/80
12	2-OMe	3l	45/76	40/73	5/77	5/80
13	3,4-OMe	3m	40/70	40/72	5/73	4/74
14	2-OH,3-OMe	3n	35/73	35/70	6/78	5/84
15	4-OH, 3-OEt	3o	35/73	40/75	5/78	5/84

<sup>a</sup> 1,8-Diaminonaphthalene (1 mmol), aldehyde (1 mmol) and nano- $\gamma$ -Al<sub>2</sub>O<sub>3</sub>/BF<sub>n</sub>/ Fe<sub>3</sub>O<sub>4</sub> (0.06, 0.06, 0.03 and 0.03g for grinding, reflux, microwave and ultrasonic methods, respectively) were used.

<sup>b</sup> Isolated yield.

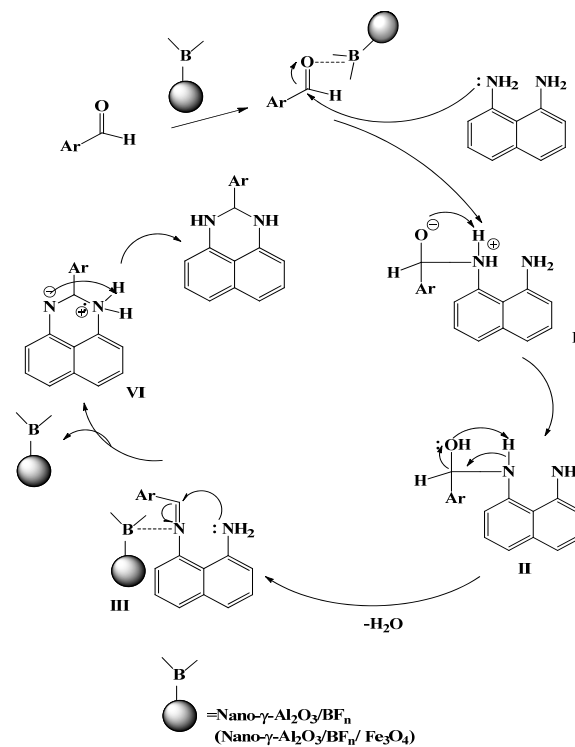


Fig. 14. Proposed mechanism for the formation of 2,3-dihydroperimidines in the presence of nano- $\gamma$ -Al<sub>2</sub>O<sub>3</sub>/BF<sub>n</sub> and nano- $\gamma$ -Al<sub>2</sub>O<sub>3</sub>/BF<sub>n</sub>/ Fe<sub>3</sub>O<sub>4</sub> catalysts

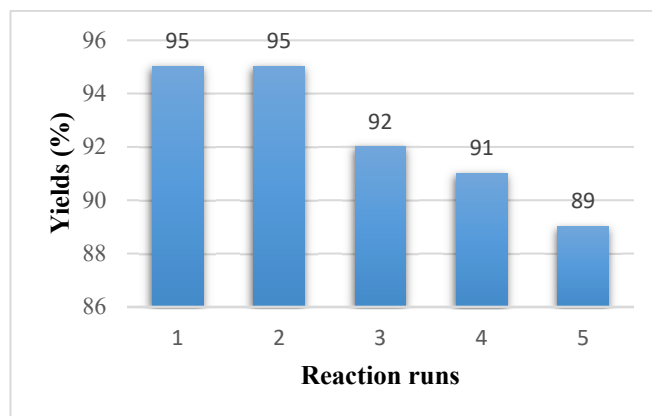


Fig. 15. Reusability of the magnetic nano catalyst

and 4-chlorobenzaldehyde ( five times with only a slight decrease in its catalytic activity (Fig. 15). Partial loss of activity may be due to blockage of active sites of the catalyst.

## CONCLUSION

In summary, we have reported a simple and ecofriendly protocol for the preparation of 2,3-dihydroperimidine derivatives by two nano acid catalysts under different conditions in good yields. These green protocols permit to synthesize a range of corresponding products in excellent yields with Short reaction times, high conversions, clean reaction profiles, simple work-up, availability and low catalyst loading in the absence of any hazardous organic solvents. As you can see in the tables 2 and 3, the magnetic catalyst nano- $\gamma$ - $\text{Al}_2\text{O}_3$ / $\text{BF}_3$ / $\text{Fe}_3\text{O}_4$  shows higher efficiency in all different methods. Also, this magnetic nano catalyst could be successfully reused at least for five runs without significant loss in its activity.

## ACKNOWLEDGMENTS

The authors are grateful to Damghan University and University of Kashan for financial support of this work.

## CONFLICT OF INTEREST

The authors declare that there are no conflicts of interest regarding the publication of this manuscript.

## REFERENCES

- Gomtsyan A. Heterocycles in Drugs and Drug Discovery. *Chemistry of Heterocyclic Compounds*. 2012; 48 (1): 7–10.
- Farghaly T. A, Abbas E. M. H, Dawood K. M, El-Naggar T. B. A. Synthesis of 2-Phenylazonaphtho[1,8-ef][1,4] Diazepines and 9-(3-Arylhrazono) Pyrrolo [1,2-a] Perimidines as
- Antitumor Agents. *Molecules*. 2014; 19 (1): 740–755.
- Dua R, Shrivastava S, Sonwane S.K, Srivastava S.K. Pharmacological Significance of Synthetic Heterocycles Scaffold: A Review. *Advances in Biological Research*. 2011; 5 (3): 120–144.
- Harry N. A, Cherian R. M, Radhika S, Anilkumar G. A novel Catalyst-Free, Eco-Friendly, on Water Protocol for the Synthesis of 2,3- dihydro-1H-Perimidines. *Tetrahedron Letters*. 2019; 60 (33):150946.
- Alam M, Lee D.-U. Synthesis, Spectroscopic and Computational Studies of 2-(thiophen-2- yl)-2,3-dihydro-1H-Perimidine: An Enzymes Inhibition Study. *Computational Biology and Chemistry*. 2016; 64:185–201.
- Azam M, Warad I, Al-Resayes S. I, Alzaqri N, Rizwan Khan M, Pallepogu R, Dwivedi S, Musarrat J, Shakir M. Synthesis and Structural Characterization of Pd (II) Complexes Derived from Perimidine Ligand and their in Vitro Antimicrobial Studies. *Journal of Molecular Structure*. 2013; 1047: 48–54.
- Sheibani H, Seifi M, Bazgir A. Three-Component Synthesis of Pyrimidine and Pyrimidinone Derivatives in the Presence of High-Surface-Area MgO, a Highly Effective Heterogeneous Base Catalyst. *Synthetic Communications*. 2009; 39: 1055–1064.
- Lin Y, Zhongyan L , Guokai J, Min Z, YUAN Xianyou Y. Synthesis and Biological Activity of Perimidine Derivatives. *Chinese Journal of Applied Chemistry*. 2017; 34 (6): 685–692.
- Kobrakov K. I, Zubkova N. S, Stankevich G.S, Shestakova Yu. S, Stroganov V. S, Adrov O. I, New Aroyleneimidazoles as Dyes for Thermoplastic Polymeric Materials, *Fibre Chemistry*. 2006; 38: 183-187.
- Bazinet P, Yap G. P. A, Richeson D. S. Constructing a Stable Carbene with a Novel Topology and Electronic Frame Work. *Journal of the American Chemical Society*. 2003; 125 (44): 13314-13315.
- Kalhor M, Khodaparast N. Use of Nano-CuY Zeolite as an Efficient and Eco-Friendly Nano Catalyst for Facile Synthesis of Perimidine Derivatives. *Research of Chemical Intermediates*. 2015; 41: 3235-3242.
- Sahiba N, Agarwal Sh. Recent Advances in the Synthesis of Perimidines and their Applications. *Topics in Current Chemistry chines*. 2020; 378 (44), DOI: 10.1007/s41061-

- 020-00307-5.
13. Mahmoodi Fard Chegeni M, Bamoniri A, Taherpour A. A. One-pot Synthesis of 2H-Indazolo[2,1-b] Phthalazine-triones via Nano  $\gamma$ -Al<sub>2</sub>O<sub>3</sub>/BF<sub>3</sub>/Fe<sub>3</sub>O<sub>4</sub> as an Efficient Catalyst and Theoretical DFT Study on them. *Journal of Heterocyclic Chemistry*. 2020; 57 (7): 2801-2814. DOI: 10.1002/jhet.3989.
  14. Bamoniri A, Mirjalili B. F., Pooladsanj S, Teymouri F. Nano Silica Gel Supported Perchloric Acid/Wet SiO<sub>2</sub>: an Efficient Reagent for one - Pot Synthesis of Azo Dyes Based on 1-Naphthol in Room Temperature and Solvent Free Conditions. *Iranian Journal of Organic Chemistry*. 2011; 3(1): 573-576.
  15. Salehi P, Zolfigol M.A, Shirini F, Baghbanzadeh M. Silica Sulfuric Acid and Silica Chloride as Efficient Reagents for Organic Reactions. *Current Organic Chemistry*. 2006; 10 (17): 2171-2189.
  16. Mobinikhaledi A, Foroughifar N, Basaki N. Zeolite Catalyzed Efficient Synthesis of Perimidines at Room Temperature. *Turkish Journal of Chemistry*. 2009; 33: 555–560.
  17. Patil V. D, Patil K. P, Sutar N. R, Gidh P.V. Phenyl Boronic Acid Promoted Efficient Synthesis of Perimidine Derivatives under Mild Condition. *Chemistry International*. 2017; 3(3): 195-201.
  18. Amrollahi M.A, Vahidnia F. Decoration of  $\beta$ -CD-ZrO on Fe<sub>3</sub>O<sub>4</sub> Magnetic Nanoparticles as a Magnetically, Recoverable and Reusable Catalyst for the Synthesis of 2,3-dihydro-1H-Perimidines. *Research on Chemical Intermediates*. 2018, 44: 7569- 7581. DOI: 10.1007/s11164-018-3574-y.
  19. Behbahani F.K., Golchin F. M. A New Catalyst for the Synthesis of 2-Substituted Perimidines Catalysed by FePO<sub>4</sub>. *Journal of Taibah University for Science*. 2017; 11: 85–89.
  20. Patil V.V, Shankarling G.S. A Metal Free, Eco-Friendly Protocol for the Synthesis of 2,3-dihydro-1H-Perimidines Using Commercially Available Amberlyst 15 as a Catalyst. *Catalysis Communications*. 2014; 57: 138–142.
  21. Phadtare S. B, Vijayraghavan R, Shankarling G. S, MacFarlane D.R. Efficient Synthesis of 2,3-Dihydro-1H-Perimidine Derivatives Using H<sub>2</sub>BOB as a Novel Solid Acid Catalyst. *Australian Journal of Chemistry*. 2012; 65 (1): 86–90.
  22. Bamoniri A, Mirjalili B. B. F, Saleh S., Nano- $\gamma$ -Al<sub>2</sub>O<sub>3</sub>/SbCl<sub>5</sub>: An Efficient Catalyst for the Synthesis of 2,3-dihydroperimidines. *RSC Advances*. 2018; 8: 6178–6182.
  23. Zhang S-L, Zhang J-M. Ytterbium (III) Triflate as an Efficient Catalyst for the Synthesis of Perimidine Derivatives under Mild Conditions. *Chinese Journal of Chemistry*. 2008; 26 (1): 185–189.
  24. Farrokhi A, Ghodrati K, Yavari I .Fe<sub>3</sub>O<sub>4</sub>/SiO<sub>2</sub>/(CH<sub>2</sub>)<sub>3</sub>N+Me<sub>3</sub>Br<sup>3-</sup> Core–Shell Nanoparticles: A novel Catalyst for the Solvent-Free Synthesis of Five- and Six-Membered Heterocycles. *Catalysis Communications*. 2015; 63: 41–46.
  25. Harry N. A, Radhika S, Neetha M, Anilkumar G. A Novel Catalyst-Free Mechanochemical Protocol for the Synthesis of 2,3-Dihydro-1H-Perimidines. *Journal of Heterocyclic chemistry*. 2020; 57 (4): 2037-2043.
  26. Bahrami K, S. Saleh S. [BTBA]Cl-FeCl<sub>3</sub> as an Efficient Lewis Acid Ionic Liquid for the Synthesis of Perimidine Derivatives. *Synthesis and Reactivity in Inorganic, Metal-Organic, and Nano-Metal Chemistry*. 2016; 46 (6). DOI: 10.1080/15533174.2014.989602.